LA-UR-73-1310

Conf-730915--4

ADSORPTION OF RADIOKRYPTON ON ACTIVATED CHARCOAL IN THE PRESENCE OF HYDROGEN

by

B. B. Fisher

A. E. Norris

D. G. Rose

Los Alamos Scientific Laboratory
of the University of California
Los Alamos, New Mexico

Introduction

The Nuclear Furnace-1 was a small test reactor which was devised to provide an inexpensive means of testing nuclear rocket fuel elements and other core components. The various runs, called Experimental Plans, which took place in the period between May 24 and July 27, 1973 were the first occasions in which the hydrogen propellant flow from a reactor rocket engine was scrubbed clean of all radioactivity before being liberated to the atmosphere by burning it in a flare stack. The last component of the effluent cleanup system (ECS) was a fixed-bed activated-charcoal trap operated at low temperatures to remove radiokrypton and radioxenon from the effluent gases. Experiments were performed to measure the velocity of the krypton adsorption front through the charcoal trap by measuring the amounts of radiokrypton upstream, downstream, and in two locations within the charcoal trap.

The following results were obtained:

1. When operated at the proper temperature the NF-1 charcoal trap removed the radiokrypton and radioxenon from the effluent stream.

2. The dynamic adsorption coefficients of krypton upon activated charcoal derived from these experiments are less than those in the literature for krypton adsorbed from helium. This effect can probably be ascribed to the fact that the hydrogen in the effluent is interfering with krypton adsorption.

3. The number of ^{89}Kr atoms entering the charcoal trap as measured by these experiments are in fair agreement with the measurements made by Nuclear Rocket Test Operations, and both agree with the computations of the amount of ^{89}Kr released by the elements.

Theory

Hydrogen effluent exiting the reactor at ∿ 2440 K was cooled by the injection of water into the effluent stream. Passing through a series of heat exchangers and water separators, the effluent was then cooled further and condensed, and the added water was removed with a large fraction of nuclides that were in particulate form or were soluble in water. After this, the effluent passed through a fixed-bed silicagel drier and through a cryogenically cooled fixed-bed activated-charcoal trap to remove the noble-gas fission products, krypton and xenon.

Xenon is adsorbed much more strongly upon activated charcoal than is krypton. Therefore, any trap designed to remove krypton from a gas stream will be more effective for xenon. This discussion will be limited to the case of the adsorption of krypton on activated charcoal, particularly North American G-212, 8x16-mesh, the type used in the charcoal trap.

When the effluent stream from the reactor reaches the inlet to the charcoal trap, the effluent consists primarily of hydrogen gas, but contains gaseous impurities that result from fuel-element corrosion and from the reaction of those corrosion products with the water added to cool the reactor effluent. It may also contain some particulate matter, which need not be considered here. Table I lists a predicted composition of the effluent stream from NF-1 at the inlet to the charcoal trap.

TABLE I

ESTIMATED NF-1 EFFLUENT COMPOSITION

Constituent	Mole Fraction	Partial Pressure, Pa
H_2	1.0	4.14×10^{5}
H_2O	7.09×10^{-7}	4.89×10^{-3}
CH_4	2.78×10^{-6}	1.92×10^{-2}
CO	8.44×10^{-7}	5.82×10^{-3}
Xe	1.54×10^{-10}	1.06×10^{-6}
Kr	7.91×10^{-11}	5.45 x 10-7

Although such impurities as CH_4 and carbon monoxide can reduce the amount of krypton adsorbed upon charcoal an examination of the literature (Burnette 1967), indicated that in the concentrations found in the NF-1 effluent stream they will not effect krypton adsorption. Water vapor is so strongly adsorbed upon charcoal as to completely prevent the adsorption of krypton or xenon, but the amount of water carried to the trap by the effluent is so low that it will poison only the first few millimeters of charcoal and effectively shorten the trap by that small length. Hydrogen is adsorbed upon activated charcoal less strongly than either krypton or xenon. However, the amount of gas adsorbed upon charcoal at any temperature will increase as the pressure of that gas is increased. What effect the hydrogen in the effluent, which is at $\sim 4\times10^{5}$ Pa, would have upon the adsorption of krypton, which is at a partial pressure of only 5.45×10^{-7} Pa, was unknown before the NF-1 tests, and this was one of the facts to be determined by the experiments.

Table II and Fig. 1 present the dynamic adsorption coefficient of krypton upon activated charcoal versus temperature for low concentrations of krypton in helium (Burnette, 1961, 1967, Kovatch 1970). These values were measured in the absence of gases that would interfere with the adsorption of the krypton.

TABLE II

DYNAMIC ADSORPTION COEFFICIENTS, K_D, FOR KRYPTON ON CHARCOAL

$1000/T\ (K^{-1})$	$K_D\ (m^3/kg)$	Ref.
3.55	0.103	3
3.62	0.127	2
3.62	0.152	2
4.0	0.229	3
4.0	0.275	1
4.35	0.488	1
4.45	0.700	3
4.60	1.195	1
5.25	5.230	1
5.65	18.150	1
5.95	135.	1
6.60	305.	1
7.00	940.	1
7.50	1953.	1

When a concentration of krypton is added at some definite time to a hydrogen stream flowing through a fixed charcoal bed the krypton travels through the bed as a concentration front which moves from the inlet to the outlet of the trap. Because the escape of fission products from the fuel elements is a very steep function of temperature, the krypton does appear in the effluent stream suddenly as the fuel elements reach their operating temperature. This front moves through the bed at a velocity that is a fraction of the velocity of the carrier hydrogen, depending upon the value of the dynamic adsorption coefficient. As the krypton concentration front moves through the charcoal bed the krypton becomes diffuse because of mass-transfer effects and diffusion. Barnette, 1961 presents an expression that allows the concentration of the krypton in a hydrogen stream flowing through an activated charcoal bed to be calculated as a function of bed conditions, time of flow, and distance through the charcoal bed (this expression includes the effect of decay if the krypton is radioactive):

$$\frac{c}{c_o} = e^{-\alpha x r/(1+r)}\left[1 - \left(\frac{1}{1+r}\right) e^{-\beta\tau(1+r)} \int_0^{\alpha x} e^{-t/(1+r)}\, I_o\left(2\sqrt{\beta\tau t}\right) dt\right],$$

$$\alpha = \frac{1}{H}, \quad \beta = \frac{LV}{\text{[illegible]}},$$

where

c_o = concentration in gas stream entering bed, moles/m^3,

V = volume flow rate of gas, m^3/s,

H = height of mass-transfer unit, m,

H can be estimated from the following expression:

$$H = \frac{0.168}{a}\left[\frac{D_p G}{\mu}\right]^{0.51}\left[\frac{\mu}{\rho D_v}\right]^{2/3}$$

where

a = superficial area of bed particles per unit volume, m^2/m^3

D_p = average particle diameter, m

G = flow rate per unit area, $kg/m^2.s$

μ = viscosity, kg/m.s

ρ = carrier gas density, kg/m^3

D_v = diffusivity of adsorbate in carrier gas, m^2/sec

c = concentration of adsorbate in gas stream, $mole/m^3$,

τ = time, sec,

x = distance along adsorber bed, m,

M = total mass of adsorbent in bed, kg,

F = void fraction in adsorber bed,

L = total length of bed, m,

λ = radioactive decay constant, s^{-1},

$r = \lambda/\beta$,

I_o = modified Bessel function of the first kind and zero order.

They found good agreement with this expression in experiments investigating the adsorption of krypton on activated charcoal from a helium stream.

The experiments carried out on the NF-1 effluent cleanup system charcoal trap involved the use of activated-charcoal sampling traps, cooled to liquid-nitrogen temperatures, which sampled the effluent upstream, downstream, and at two positions within the large charcoal trap. The sampling traps, operating at much lower temperatures than the large trap, are much more efficient and are able to remove all the krypton and xenon from the effluent. These traps integrate the concentration of ^{89}Sr, ^{88}Kr, and $^{85}Kr^m$ in the effluent over the time of the reactor run. For comparison with the experimental results the integral of c/c_o was computed for each sampling trap in each experimental plan. The computations were done by using the proper temperature of operation of the large charcoal trap and length of run for each experimental plan. In addition, because the effect of hydrogen upon the adsorption of krypton is uncertain, the computation was performed by using a dynamic adsorption coefficient equal to 1, 1/2, 1/3, 1/5, 1/7, and 1/10 the literature value for krypton adsorption upon charcoal. The results of these computations as well as the experimental results are discussed below.

Experimental

The charcoal trap of the NF-1 effluent cleanup system has a diameter of 1.52 m and is filled to a depth of 1.8 m with 1565 kg of North American Type G-212 activated charcoal of 8x16-mesh particle size.

The experiments were planned to measure the velocity of the krypton concentration front through the fixed charcoal trap by sampling the effluent in the charcoal trap at four locations. To do this, four bypass lines were installed in and around the large charcoal trap to lead small fractions of the effluent flow to the sampling traps. Figure 2 presents a schematic of the sampling system. The identifications and locations of the sampling positions are given below:

TRAP 20 - immediately upstream from the large trap.

TRAP 30 - 0.152 m below the charcoal inlet surface.

TRAP 40 - 0.762 m below the charcoal inlet surface,

TRAP 50 - at outlet from charcoal trap; this is equivalent to 1.8 m below the charcoal inlet surface.

The effluent sampling head placed in the charcoal trap itself consisted of 0.5-in. stainless-steel tubing, which was capped at the end and which had holes of ~ 9.5 mm diam drilled into the sides of the tube at such positions that gas flow was taken from 0.152, 0.244, and 0.337 m from the center line of the charcoal trap. The holes were covered with 20-mesh wire screen to exclude charcoal from the bypass lines. The samples upstream and downstream of the charcoal trap were taken through 1.0-in. pipes which led from the main effluent piping. The effluent flow through each of the sampling traps, amounting to 6.3×10^{-4} m^3/sec, was led directly to the flare-stack header. The effluent flow to be analyzed was taken from the bypass and put through the sampling traps which collected the radiokrypton. The flow in the bypass line and in the lines leading to the sampling traps were adjusted so that the time of flow from the large charcoal trap to the small sampling traps would all be equal and less than 30 sec.

Each sampling line had associated with it the following hardware: (1) a solenoid valve to allow the sampling flow to be saturated and stopped at a definite time, (2) a heater to warm the cold effluent, (3) a manual valve for flow control, (4) a floating ball-type flow-meter, (5) a cooling coil to cool the effluent before it entered the sampling traps, (6) the sampling traps, (7) a heater to warm the cold effluent, and (8) a check valve to prevent accidental backflow through the sampling traps.

Each sampling trap consisted of two sections in series. The upstream section (called FRONT) and the downstream section (called REAR) were of the same shape and size, a right circular cylinder 0.203 m in diameter by 0.146 m deep. They each contained 2.132 kg charcoal.

The bypass and sampling system without the flowmeters was first operated during EP-II, but so little radioactivity was found in the sampling traps that there was doubt that any flow had taken place through the sampling system. To ensure bypass flow through the sampling traps for EP-III and succeeding runs, the following changes were made: (1) the 0.250-in. tubing in the liquid-nitrogen bath immediately ahead of each sampling trap was changed to 0.5-in. tubing, to help prevent formation of ice blockage should any water enter the system; (2) the flowmeters shown in Fig. 2 were installed in the outlet line from each trap, just upstream from the check valve; a television camera was used to view the flowmeters during the reactor runs; (3) a wet test meter was used to calibrate the flowmeter before EP-III and EP-V but not before EP-IV. Helium had to be used for the calibrations and the response of the flowmeters to hydrogen flow had to be calculated. This computation was performed by NRTO. The calibration data were combined with the flowmeter readings observed during each reactor run to obtain the rates of flow for each sampling trap during each experimental plan. The results are shown in Table III.

Of necessity, the flow calibrations were carried out rather crudely in the field, which leads one to expect that the largest source of error in the results of the measurements arises from uncertainties in the flow measurements. Before each reactor run the small traps were filled with North American Carbon Type G-212 activated charcoal 8x16-mesh, sealed, pressure-tested, and the charcoal was regenerated by a flow of hot N_2 for 86.4 ksec. During installation of the traps care was taken to minimize the atmospheric water that could enter the piping.

On the day following each reactor run, the sampling traps were removed from Test Cell-C to the core sample building at the Nevada Test Site, where the charcoal in each trap was thoroughly mixed and aliquots taken. One aliquot was used for γ-ray spectrometric measurements and the other was sent to LASL for radiochemical analysis of ^{89}Sr. The γ-ray spectroscopy measurements were made with a 16×10^3 mm^3 Ge(Li) detector at NRDS.

TABLE III

HYDROGEN FLOW DATA

	TRAP 20	TRAP 30	TRAP 40	TRAP 50
Hydrogen flow rate computed, from wet testmeter results before EP-III	4.18×10^{-4} m³/s	4.2×10^{-4} m³/s	4.18×10^{-4} m³/s	3.85×10^{-4} m³/s
Flow gage level computed for H_2[a]	0.35	0.305	15.6	0.24
EP-III observed flow gage level[a]	0.30	0.30	25.0	0.2
Computed H_2 flow rate	3.58×10^{-4} m³/s	4.13×10^{-4} m³/s	6.69×10^{-4} m³/s	3.21×10^{-4} m³/s
Normalization factor	1.000	0.866	0.535	1.115
EP-IV observed flow gage level[a]	0.3	0.2	10.0	0.10
Computed H_2 flow rate	3.58×10^{-4} m³/s	2.75×10^{-4} m³/s	2.68×10^{-4} m³/s	1.60×10^{-4} m³/s
Normalization factor	1.000	1.300	1.337	2.232
Hydrogen flow rate computed from wet testmeter results before EP-V	4.18×10^{-4} m³/s	4.1×10^{-4} m³/s	3.88×10^{-4} m³/s	2.28×10^{-4} m³/s
Flow gage level computed for H_2[a]	0.38	0.32	16.0	0.25
EP-V observed flow gage level[a]	0.47	0.33	15.0	0.19
Computed H_2 flow rate	5.17×10^{-4} m³/s	4.23×10^{-4} m³/s	3.64×10^{-4} m³/s	1.73×10^{-4} m³/s
Normalization factor	1.000	1.224	1.421	2.990

[a] Arbitrary scale.

Results and Conclusions

Only the final ratios of activities in the various traps are presented below.

Gamma Ray Spectroscopy

Table IV gives the ratios of the activities of $^{85}Kr^{m}$ and ^{88}Kr in Traps 30, 40, and 50 to that found in Trap 20, as measured by γ-spectroscopy. The specific γ-ray peaks that were integrated for these results are the 151.1-keV peak for $^{85}Kr^{m}$, and the 196.1-keV peak for ^{88}Kr. The data have been corrected for radioactive decay, for branching ratios, for sample mass, and for detector efficiency. The detector efficiency was measured with an I.A.E.A.-calibrated ^{22}Na source imbedded in an appropriate mass of inactive charcoal. Inaccuracies in the absolute measurement of the detector efficiency cancel in the ratios.

TABLE IV

GAMMA-RAY SPECTROSCOPY RESULTS

	EP-III		EP-IV		EP-V	
	$^{85}Kr^{m}$	^{88}Kr	$^{85}Kr^{m}$	^{88}Kr	$^{85}Kr^{m}$	^{88}Kr
TRAP 30/TRAP 20	4.1×10^{-2}	6.27×10^{-2}	6.5×10^{-1}	7.57×10^{-1}	8.34×10^{-1}	8.37×10^{-1}
TRAP 40/TRAP 20	--	--	9.86×10^{-6}	--	5.96×10^{-1}	5.57×10^{-1}
TRAP 50/TRAP 20	--	--	--	--	4.24×10^{-1}	4.27×10^{-1}

A potentially important source of error in these γ-ray measurements results from the gradual desorption of krypton from charcoal at room temperature while the samples are being counted. One indication that krypton was being lost from the samples during the process of γ-ray counting comes from measurements taken on Trap 30 from EP-IV. Triplicate aliquots of charcoal from the front cannister of Trap 30 were taken to measure the uniformity of sampling. The activity of each sample, corrected for mass and forradioactive decay, monotonically decreased with the order in which the samples were counted. The same three aliquots were analyzed for ^{89}Sr, and no such monotonic decrease in activity was observed. The plastic bottles that served as containers for the charcoal during γ-ray counting were not gas-tight. In Table IV only the data from the aliquot that was counted first are shown.

In all cases except for EP-V, the quantities of ^{135}Xe, which was measured in the small traps, was higher in the downstream portion of the traps than in the upstream portion. In addition, the complete absence of ^{135}Xe in EP-III Trap 30 and its presence in Traps 20, 40, and 50 indicated that the ^{135}Xe might be entering the traps other than in the normal way. Also in EP-III the Trap-40 and Trap-50 data indicated significant quantities of $^{85}Kr^{m}$ and ^{88}Kr in the downstream portions of these traps. The probability that the data from Trap 40 and Trap 50 were compromised by extraneous effects is sufficiently high that no further use will be made of these data. The check valve in each bypass line was replaced before EP-IV, and the situation seemed to improve. The check valves were replaced again before EP-V and further improvement was noticed, although the ^{135}Xe detected in EP-V Trap 50 indicated that some small problem remained.

^{89}Sr Analyses

The results of the ^{89}Sr measurements are shown in Table V. The principal source of error is likely to be uncertainties in the actual flow of H_2 through each of the sampling traps and the problem of backflow in the traps. The ratios shown in parentheses for EP-III were derived by considering only the activities in the upstream portion of the sampling trap; all other ratios are formed by summing the activities in the upstream and downstream portion of each sampling trap.

Sampling-trap activities as calculated and as measured are compared in Tables VI through XII. From such a comparison an estimate of the effective velocity of travel of the concentration front or, alternatively, the effective dynamic adsorption coefficient can be obtained. Table XIII gives the estimates of the velocity factors thus obtained. Note that the ^{88}Kr and $^{85}Kr^{m}$ results, although suspect, do not disagree seriously with the ^{89}Sr data.

TABLE V

^{89}Sr ANALYSES RESULTS

	EP-III	EP-IV	EP-V
TRAP 30/TRAP 20	5.27×10^{-2}	3.26×10^{-1}	3.18×10^{-1}
TRAP 40/TRAP 20	1.06×10^{-3} (1.1×10^{-4})	4.42x10-5	4.82×10^{-2}
TRAP 50/TRAP 20	2.7×10^{-3} (6.5×10^{-4})	7.73×10^{-5}	1.31×10^{-3}

TABLE VI

COMPARISON OF COMPUTED AND MEASURED
SAMPLING TRAP ACTIVITY RATIOS OF ^{89}Sr FOR EP-III

Trap Pair	Velocity Factor						Measured Ratio
	1	2	3	5	7	10	
$\frac{730}{720}$	10^{-5}	0.001	0.006	0.053	0.146	0.296	0.053
$\frac{740}{720}$	10^{-30}	10^{-25}	10^{-22}	10^{-18}	10^{-13}	10^{-9}	---
$\frac{750}{720}$	10^{-76}	10^{-68}	10^{-63}	10^{-54}	10^{-47}	10^{-40}	---

TABLE VII

COMPARISON OF COMPUTED AND MEASURED
SAMPLING TRAP ACTIVITY RATIOS OF ^{89}Sr FOR EP-IV

Trap Pair	Velocity Factor						Measured Ratio
	1	2	3	5	7	10	
$\frac{730}{720}$	10^{-4}	0.004	0.016	0.066	0.133	0.233	0.326
$\frac{740}{720}$	10^{-22}	10^{-16}	10^{-12}	10^{-7}	10^{-9}	10^{-4}	10^{-5}
$\frac{750}{720}$	10^{-58}	10^{-50}	10^{-42}	10^{-30}	10^{-40}	10^{-14}	10^{-4}

TABLE VIII

COMPARISON OF COMPUTED AND MEASURED
SAMPLING TRAP ACTIVITY RATIOS OF ^{89}Sr FOR EP-V

Trap Pair	Velocity Factor						Measured Ratio
	1	2	3	5	7	10	
$\frac{730}{720}$	0.208	0.450	0.580	0.709	0.773	0.826	0.318
$\frac{740}{720}$	10^{-4}	0.016	0.061	0.182	0.302	0.443	0.048
$\frac{750}{720}$	10^{-13}	10^{-5}	0.001	0.016	0.053	0.131	0.001

TABLE IX

COMPARISON OF COMPUTED AND MEASURED
SAMPLING TRAP ACTIVITY RATIOS OF ^{88}Kr FOR EP-III

Trap Pair	Velocity Factor						Measured Ratio
	1	2	3	5	7	10	
$\frac{730}{720}$	10^{-4}	0.002	0.012	0.089	0.233	0.435	0.063
$\frac{740}{720}$	10^{-29}	10^{-25}	10^{-22}	10^{-17}	10^{-13}	10^{-9}	--
$\frac{750}{720}$	10^{-76}	10^{-68}	10^{-62}	10^{-53}	10^{-47}	10^{-40}	--

TABLE X

COMPARISON OF COMPUTED AND MEASURED
SAMPLING TRAP ACTIVITY RATIOS OF ^{88}Kr FOR EP-IV

Trap Pair	Velocity Factor						Measured Ratio
	1	2	3	5	7	10	
$\frac{730}{720}$	0.021	0.212	0.427	0.644	0.743	0.819	0.757
$\frac{740}{720}$	10^{-20}	10^{-13}	10^{-8}	10^{-4}	0.014	0.170	--
$\frac{750}{720}$	10^{-58}	10^{-46}	10^{-38}	10^{-26}	10^{-19}	10^{-10}	--

TABLE XI

COMPARISON OF COMPUTED AND MEASURED
SAMPLING TRAP ACTIVITY RATIOS OF ^{88}Kr FOR EP-V

Trap Pair	Velocity Factor						Measured Ratio
	1	2	3	5	7	10	
$\frac{730}{720}$	0.838	0.939	0.956	0.960	0.961	0.963	0.837
$\frac{740}{720}$	0.258	0.604	0.729	0.828	0.888	0.951	0.557
$\frac{750}{720}$	10^{-8}	0.131	0.389	0.616	0.720	0.819	0.427

TABLE XII

COMPARISON OF COMPUTED AND MEASURED SAMPLING TRAP ACTIVITY RATIOS OF $^{85}Kr^{m}$ FOR EP-V

Trap Pair	Velocity Factor 1	2	3	5	7	10	Measured Ratio
$\frac{730}{720}$	0.847	0.944	0.959	0.962	0.963	0.964	0.834
$\frac{740}{720}$	0.271	0.621	0.742	0.837	0.895	0.956	0.596
$\frac{750}{720}$	10^{-8}	0.140	0.406	0.632	0.733	0.830	0.424

TABLE XIII

CHARCOAL TRAP VELOCITY FACTORS FOR VARIOUS ISOTOPES

Temperature, K	Velocity Factor for Isotope[a] ^{89}Sr	^{88}Kr	$^{85}Kr^{m}$
161 (EP-IV)	~14	7.2	5
172 (EP-III)	5	4	4
186 (EP-V)	1.6	1	0.95
	2.5	1.6	1.6
	3.0	3.2	3.2

[a] The velocity factor is the ratio of the krypton front velocity found in this work divided by the velocity reported in Burnette.

The dynamic adsorption coefficients obtained from these ratios are plotted in Fig. 1. They fell below the measured line for the adsorption of krypton from helium onto activated charcoal. This decreased dynamic adsorption coefficient may be caused by the hydrogen in the effluent, decreasing the amount of krypton adsorbed.

Independent measurements of the amount of ^{89}Kr entering and leaving the large charcoal trap were made during EP-IV and EP-V by NRTO under the technical direction of SNSO-X. In Table XXVI, the values labelled NRTO were obtained by analyses of gas samples taken upstream and downstream of the charcoal trap during EP-IV and EP-V. The values labelled LASL were measured by adsorption of the ^{89}Kr in cooled charcoal traps as described above. All values were corrected for aliquots taken, counter efficiencies, flow inequalities, and decay from the time of shutdown of each EP.

TABLE XXVI

^{89}Kr ATOMS IN AND OUT OF CHARCOAL TRAP

	EP-IV (2628 sec)			EP-V (3078 sec)		
Source	In	Out	Fractional Throughput	In	Out	Fractional Throughput
NRTO	2.22×10^{19}	1.9×10^{16}	0.00086	3.22×10^{19}	1.9×10^{16}	0.00059
LASL	8.25×10^{19}	1.421×10^{16}	0.00017	1.476×10^{20}	5.77×10^{17}	0.0039

Although the number of ^{89}Kr atoms in and out of the trap in EPs-IV and -V as measured by the two methods are in fair agreement, differing only by at most a factor of 4, there is an anomaly in the NRTO data. Their measurements show the same amount of ^{89}Kr released by the trap in both experimental plans, and this makes the calculated throughput less for EP-V than for EP-IV. Because the charcoal trap was operated during EP-V at a higher temperature and for a longer time this result is most improbable. Perhaps the NRTO data have been compromised by a sneak source of activity as some of the LASL data were.

References

R. D. Burnette, W. W. Graham III, and D. G. Morse, 1961, The Removal of Radioactive Krypton and Xenon from a Flowing Helium Stream by Fixed-Bed Adsorption, Report GA-2395.

R. D. Burnette and D. R. Lofing, 1967, Low Temperature Adsorption Studies for the PSC Reactor, Report GA-7932.

J. Louis Kovatch, 1970, Krypton-Xenon Adsorption Studies on Nacar Carbons, Report NACAR-10004.

Figure 1

Dynamic Adsorption Coefficients of Krypton on Charcoal

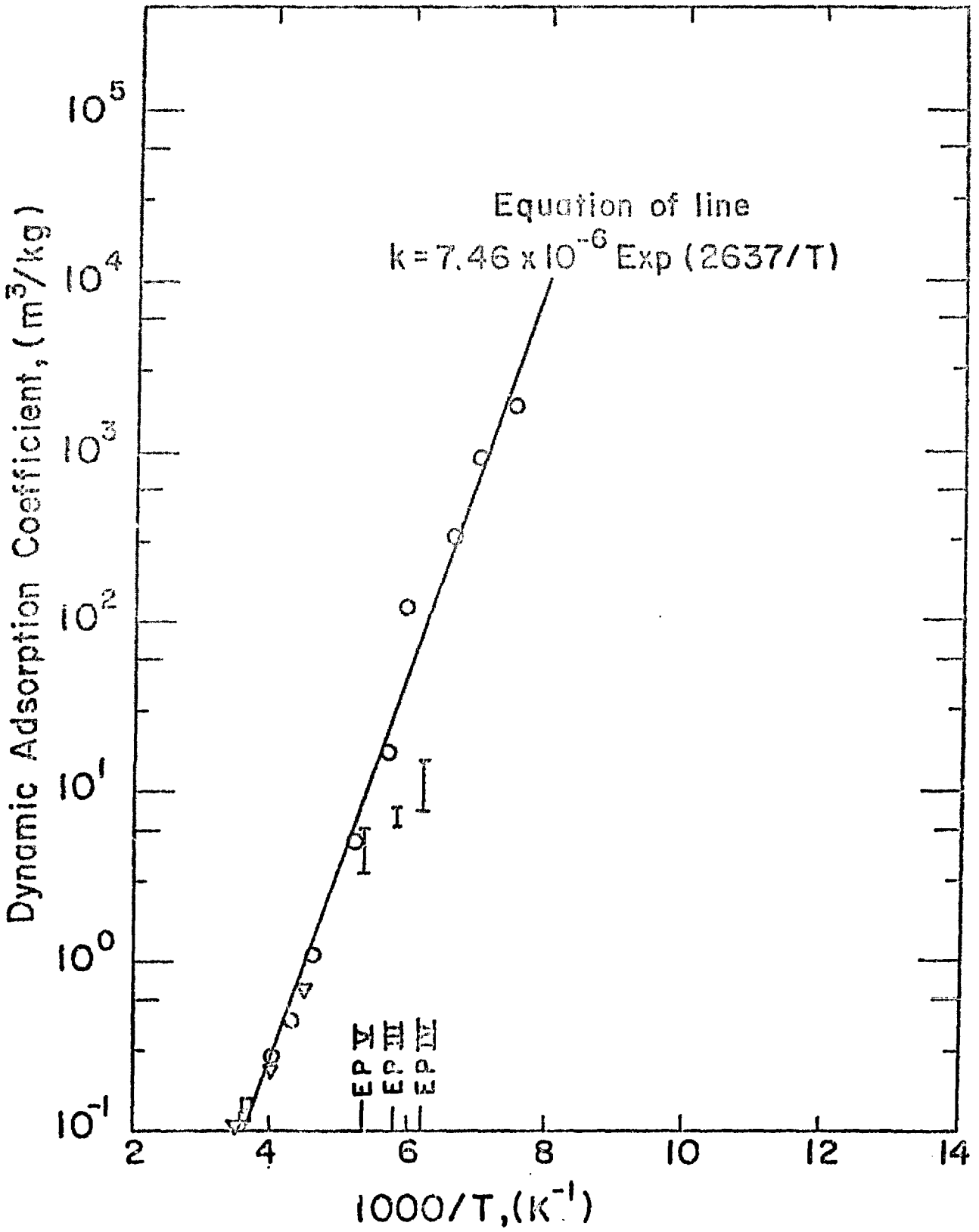
Equation of line
k = 7.46 x 10^-6 Exp (2637/T)
Dynamic Adsorption Coefficient, (m³/kg)
10⁵
10⁴
10³
10²
10¹
10⁰
10⁻¹
2
4
6
8
10
12
14
1000/T, (K⁻¹)
EP
E
E

Figure 2

NF-1 Charcoal Trap Sampling System

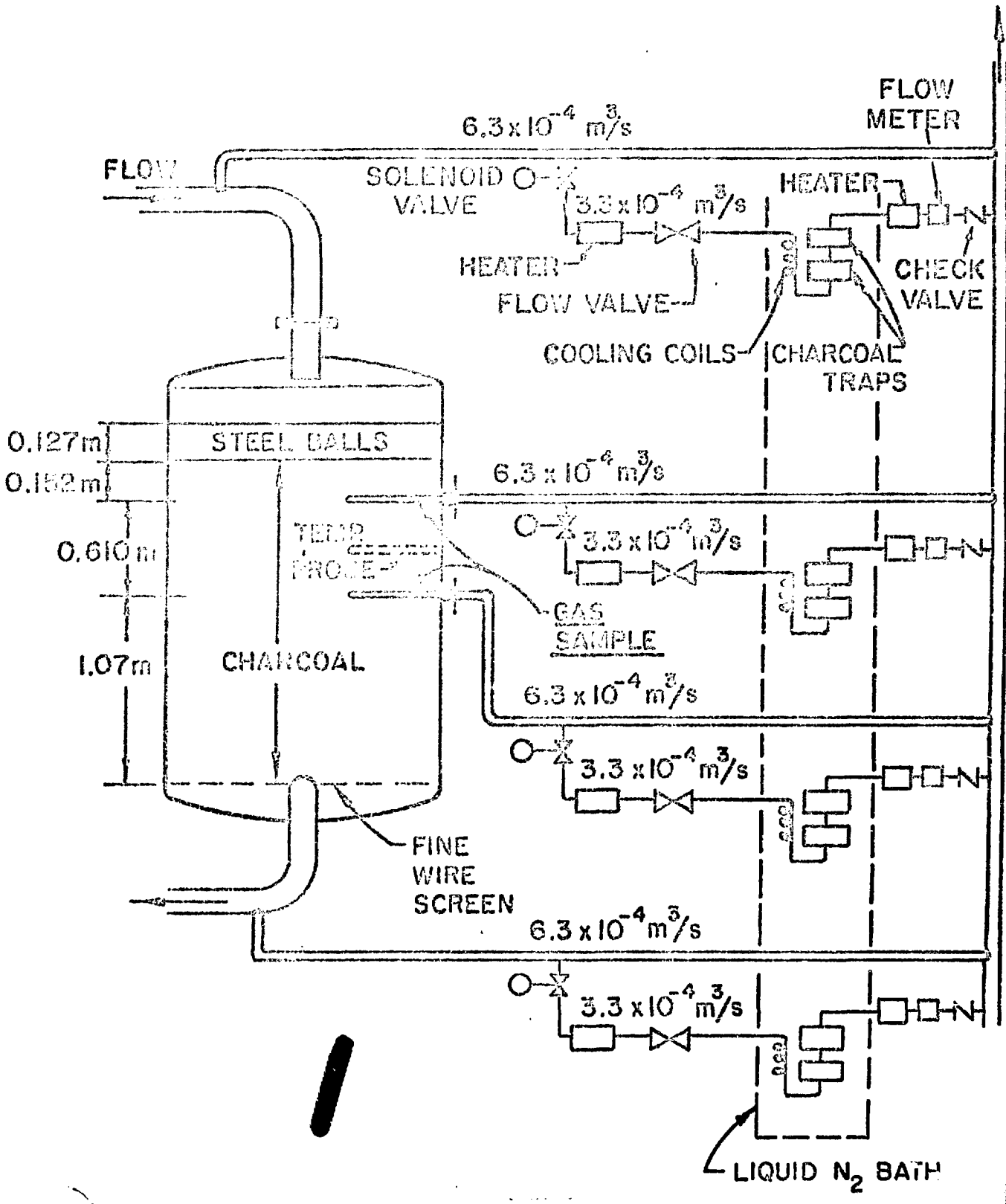

NF-1 CHARCOAL TRAP SAMPLING SYSTEM

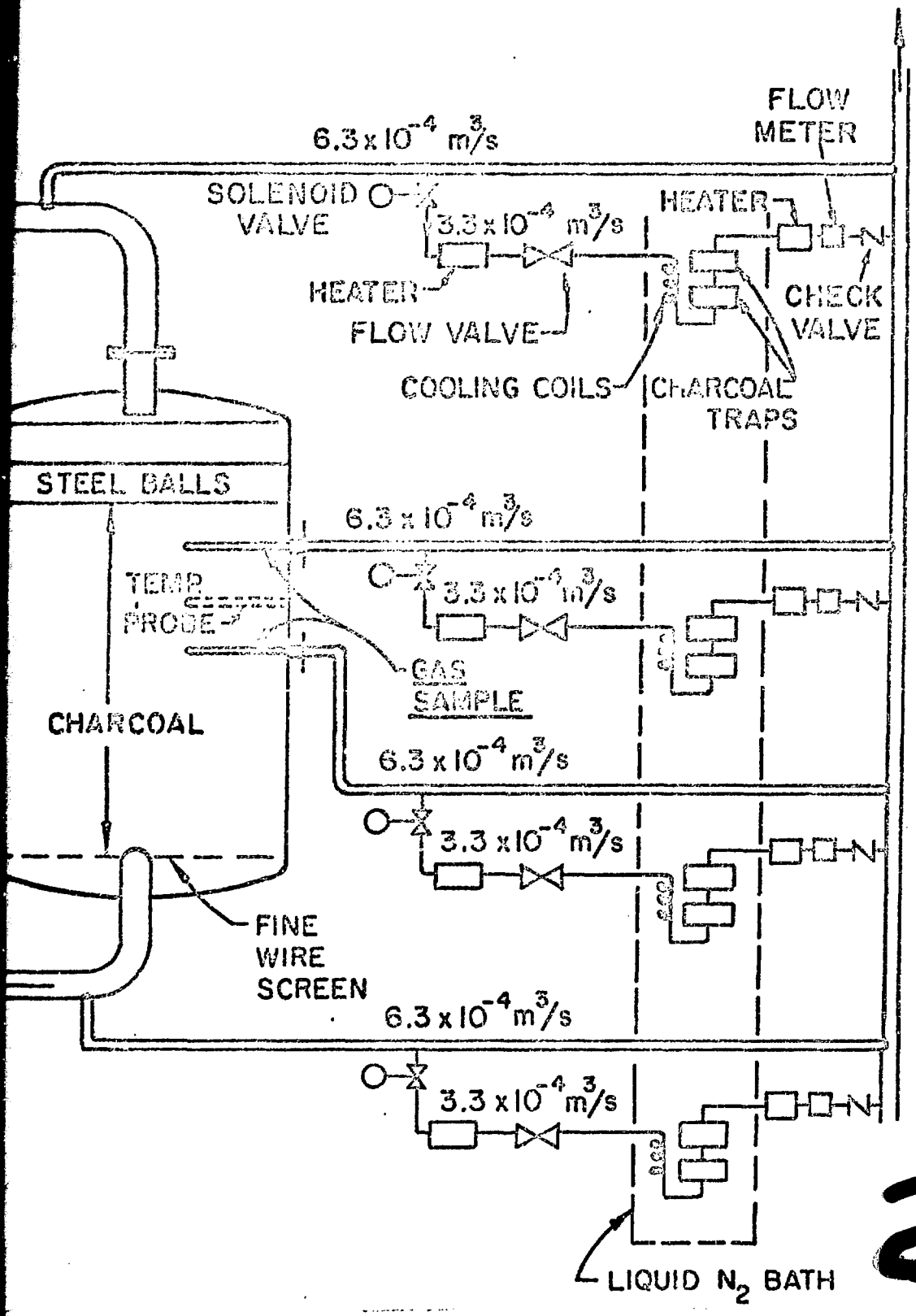

2

F-1 CHARCOAL TRAP SAMPLING SYSTEM